

Measuring anisotropies in the PTA band with cross-correlations

Giulia Cusin,^{1,2,*} Cyril Pitrou,^{1,†} Martin Pijnenburg,^{2,‡} and Alberto Sesana^{3,4,5,§}

¹*Institut d'Astrophysique de Paris, UMR-7095 du CNRS et de Sorbonne Université, Paris, France*

²*Département de Physique Théorique and Center for Astroparticle Physics,*

Université de Genève, Quai E. Ansermet 24, CH-1211 Genève 4, Switzerland

³*Dipartimento di Fisica "G. Occhialini", Università degli Studi di Milano-Bicocca, Piazza della Scienza 3, I-20126 Milano, Italy*

⁴*INFN, Sezione di Milano-Bicocca, Piazza della Scienza 3, 20126 Milano, Italy*

⁵*INAF - Osservatorio Astronomico di Brera, via Brera 20, I-20121 Milano, Italy*

(Dated: February 25, 2025)

The astrophysical gravitational wave background in the nanohertz (nHz) band is expected to be primarily composed of the superposition of signals from binaries of supermassive black holes. The spatial discreteness of these sources introduces shot noise, which, in certain regimes, would overwhelm efforts to measure the anisotropy of the gravitational wave background. In this work, we explicitly demonstrate, starting from first principles, that cross-correlating a gravitational wave background map with a sufficiently dense galaxy survey can mitigate this issue. This approach could potentially reveal underlying properties of the gravitational wave background that would otherwise remain obscured. We quantify the shot noise level and show that cross-correlating the gravitational wave background with a galaxy catalog improves by more than two orders of magnitude the prospects for a first detection of the background anisotropy by a gravitational wave observatory operating in the nHz frequency range, provided it has sufficient sensitivity.

I. INTRODUCTION

Pulsar Timing Arrays (PTAs) were used to provide the first evidence of a stochastic gravitational wave (GW) background in the nHz band [1–4], with an integrated energy density of $\Omega_{\text{GW}} = 9.3_{-4.0}^{+5.8} \cdot 10^{-9}$ [1] and evidence of spatial correlation among different pulsar redshifts following the Hellings-Downs (HD) function. Various detection methods are reviewed in [5], and the physical interpretation of the HD correlation is discussed in [6–9]. Methods for mapping the background have also been developed [10–13] (see also [14, 15] for a discussion of polarization with Stokes parameters), and it has recently been proposed that a loud source may account for the evidence of anisotropy reported in [16]. The most recent analysis of the HD signature by NANOGrav [17] is expressed in multipole space (see [18–27] for a harmonic formulation of the HD correlation), with a clear detection of the quadrupole and only marginal evidence for the octupole. The significance of background detection is expected to improve in the future, as the signal-to-noise ratio (SNR) of PTA observables increases with observation time [22, 28, 29].

The origin of the signal is still uncertain, with anisotropies in energy density providing a key observable to pin down its nature. In fact, while the overall GW signal generated by an astrophysical population of sources will inevitably show some degree of anisotropy, a cosmological background sourced in the early Universe is expected to be isotropically distributed (at least at angular scales of tens of degrees, probed by PTAs). Current sky bounds are set by NANOGrav [30], while [12] uses Fisher Information Matrix forecasts to show that sensitivity to angular power spectra improves rapidly with the number

of pulsars monitored, expected to increase by 20–40 per year.

The astrophysical gravitational wave background (AGWB) in the frequency band targeted by PTA experiments is expected to be primarily dominated by signals from binary systems of massive black holes (BBH) in the inspiraling phase [31–33]. Although the duration of these signals is exceedingly long compared to typical observation times, making the resulting background effectively continuous and stationary over the observation period (but see [34]), the sources themselves have a discrete spatial distribution. The number of sources fluctuates according to a Poisson distribution, introducing shot noise into the angular power spectrum. Additionally, sources are located in galaxies, hence they are expected to be a biased tracer of the large-scale structure distribution. In certain situations, shot noise can obscure or dominate the clustering component, making it challenging to isolate the underlying anisotropic structure of the AGWB spectrum. For example, [13] recently showed using numerical simulations that the auto-correlation map is Poisson-noise dominated, for the black hole models used in the analysis.

Cross-correlating a shot noise dominated background map with a dense galaxy map has been proved to be an effective method to alleviate shot noise limitation in the context of Earth-based detectors, where the Poissonian nature of sources is both spatial and temporal, due to the very short emission duration of mergers in band [35–40]. In particular, in [37] it is shown, in the context of ground-based detectors and considering an ideal scenario where shot noise is the only noise component, that the SNR of the cross-correlation outperforms that of the auto-correlation by several orders of magnitude.

In a similar spirit, we aim here to explore the shot noise problem in the context of PTA observations, in isolation from other sources of noise. After having identified the observables we are interested in in section II A, we present a first principle derivation of the shot noise contribution of auto- and cross-correlation maps for an AGWB in the nHz band. We need to account for two distinct layers of stochasticity describ-

* cusin@iap.fr

† pitrou@iap.fr

‡ martin.pijnenburg@unige.ch

§ alberto.sesana@unimib.it

ing the distribution of massive black hole binaries: a given galaxy may or not contain a massive black hole binary, and galaxies are themselves a discrete and random biased sampling of the underlying matter density. Using properties of compound statistics, we show that while the shot noise of the auto-correlation map is proportional to the inverse number of sources (black hole binaries), the cross-correlation shot noise is proportional to the inverse galaxy number, hence it is much suppressed. In section III we present numerical results: we consider the theoretical framework of [41–43] to describe anisotropies and we consider the astrophysical models of [44, 45] to describe the underlying massive black hole population. The AGWB strain map is dominated by a few very bright sources which obscure a background from an unresolved population, whose anisotropy map is a representative sample of large scale structure anisotropies. We therefore consider the effect of filtering out bright sources, for three different threshold values of source strain: a threshold corresponding to the EPTA strain curve (“no cut” situation as effectively there are no resolvable sources resulting from the filtering procedure), a threshold corresponding to the projected SKA strain sensitivity, and an intermediate value. For each situation we compute the auto and cross-correlation spectrum with galaxy distribution, and the corresponding shot noise contributions. We estimate the SNR of auto- and cross-correlation maps, showing that cross-correlation outperforms of more than two orders of magnitude the results of the auto-correlation alone, resulting in a potentially detectable amplitude of anisotropies. With a threshold to resolve individual events of the order 10^{-16} , detectability could be achieved by integrating the background signal over frequencies and combining the first multipoles of the background energy density, up to $\ell_{\max} = 4$. This approach requires a number of pulsars greater than $(\ell_{\max} + 1)^2 \approx 25$, which is less than the number of pulsars already monitored by single PTA collaborations.

We stress that all results reported should be understood as forecasts for a perfect experiment with no instrumental noise. As such, they represent the best-case scenario for the detectability of the AGWB in the presence of spatial shot noise. In our analysis, the entire redshift distribution of galaxies is utilized, employing optimal Wiener weights, hence assuming that the redshift distribution of GW sources is known.

II. GENERAL CONCEPTS AND DERIVATIONS

A. Our observables

The observed GW energy density parameter, Ω_{GW} is defined as the background energy density ρ_{GW} per units of logarithmic frequency f and solid angle \mathbf{n} , normalized by the critical density of the Universe today ρ_c . It can be divided into an isotropic background contribution $\bar{\Omega}_{\text{GW}}$ and a contribution from anisotropic perturbations $\delta\Omega_{\text{GW}}$ [38, 41, 42]:

$$\Omega_{\text{GW}}(\mathbf{n}, f) = \frac{f}{\rho_c} \frac{d^3 \rho_{\text{GW}}}{d^2 \mathbf{n} df}(\mathbf{n}, f) = \frac{\bar{\Omega}_{\text{GW}}(f)}{4\pi} + \delta\Omega_{\text{GW}}(\mathbf{n}, f), \quad (1)$$

where the isotropic background spectrum can be written as the integral over conformal distance r (where we set the speed of light equal to unity, $c = 1$):

$$\bar{\Omega}_{\text{GW}}(f) = \int dr \partial_r \bar{\Omega}_{\text{GW}}(f, r), \quad (2a)$$

where the integrand plays the role of an astrophysical kernel that contains information on the local production of GWs at galaxy scales. This Kernel can be built out of a model of black holes formation, or a catalog implementing such model, as detailed in Appendix C. Different astrophysical models give quite different predictions for this kernel, see e.g. [38] for an explorative approach in the frequency band of earth-based and space-based detectors.

We now consider observables integrated over the whole frequency range a given observatory is sensitive to. Explicitly, we introduce

$$\bar{\Omega}_{\text{GW}} = \int d \log f \bar{\Omega}_{\text{GW}}(f), \quad (3a)$$

$$\Omega_{\text{GW}}(\mathbf{n}) = \int d \log f \Omega_{\text{GW}}(\mathbf{n}, f), \quad (3b)$$

$$\partial_r \bar{\Omega}_{\text{GW}}(r) = \int d \log f \partial_r \bar{\Omega}_{\text{GW}}(f, r), \quad (3c)$$

$$\delta\Omega_{\text{GW}}(\mathbf{n}) = \int d \log f \delta\Omega_{\text{GW}}(\mathbf{n}, f). \quad (3d)$$

We observe that since $\delta\Omega_{\text{GW}}$ is a stochastic quantity, it can correlate with other cosmological stochastic observables. An interesting observable to look at is the cross-correlation of the AGWB with the distribution of galaxies, i.e. with the galaxy number counts Δ defined as the overdensity of the number of galaxies per unit of redshift and solid angle

$$\Delta(\mathbf{n}, z) \equiv \frac{N(z, \mathbf{n}) - \bar{N}(z)}{\bar{N}(z)}. \quad (4)$$

First, if astrophysical GW sources are located in galaxies, we would expect the SGWB and the galaxy distribution to have a high correlation level. Second, cross-correlating with galaxies helps to mitigate the problem of shot noise and to possibly extract the clustering information out of the shot noise threshold. This has been shown in the context of ground-based detectors, where shot noise is dominated by its popcorn component due to the transient emission of sources, see [35–38].

We want to show that this is also the case when the emission is continuous in time, like in the PTA band. Finally, by cross-correlating with the galaxy distribution at different redshifts, one could try to get a tomographic reconstruction of the redshift distribution of sources. In this work, our goal is to maximize the detection chances hence we do not follow this approach.

The angular power spectrum of the GW and galaxy counts auto-correlations and for their cross-correlations are defined

as

$$(2\ell + 1)C_\ell^{\text{GW}} \equiv \sum_{m=-\ell}^{\ell} \langle a_{\ell m} a_{\ell m}^* \rangle, \quad (5a)$$

$$(2\ell + 1)C_\ell^\Delta \equiv \sum_{m=-\ell}^{\ell} \langle b_{\ell m} b_{\ell m}^* \rangle, \quad (5b)$$

$$(2\ell + 1)C_\ell^{\text{GW}\Delta} \equiv \sum_{m=-\ell}^{\ell} \langle a_{\ell m} b_{\ell m}^* \rangle, \quad (5c)$$

where the bracket denotes an ensemble average and $a_{\ell m}$ and $b_{\ell m}$ are the coefficients of the spherical harmonics decomposition of the AGWB energy density and galaxy number counts, respectively. Explicitly

$$\delta\Omega_{\text{GW}}(\mathbf{n}) = \sum_{\ell=0}^{\infty} \sum_{m=-\ell}^{\ell} a_{\ell m} Y_{\ell m}(\mathbf{n}), \quad (6a)$$

$$\Delta(\mathbf{n}) = \sum_{\ell=0}^{\infty} \sum_{m=-\ell}^{\ell} b_{\ell m} Y_{\ell m}(\mathbf{n}). \quad (6b)$$

It can be shown that the angular power spectra of the auto- and cross-correlation are given by [42]:

$$C_\ell^{\text{GW}} = \frac{2}{\pi} \int dk k^2 |\delta\Omega_{\text{GW},\ell}(k)|^2, \quad (7a)$$

$$C_\ell^\Delta = \frac{2}{\pi} \int dk k^2 |\Delta_\ell(k)|^2, \quad (7b)$$

$$C_\ell^{\text{GW}\Delta} = \frac{2}{\pi} \int dk k^2 \delta\Omega_{\text{GW},\ell}^*(k) \Delta_\ell(k), \quad (7c)$$

where k is the Fourier mode norm. Keeping only the leading-order contribution to the anisotropy given by clustering, which is expressed by (C10), we have

$$\delta\Omega_{\text{GW},\ell}(k) = \int d \log f \delta\Omega_{\text{GW},\ell}(k, f), \quad (8)$$

$$\delta\Omega_{\text{GW},\ell}(k, f) = \int \frac{dr}{4\pi} \partial_r \bar{\Omega}_{\text{GW}}(f, r) [b(r) \delta_{m,k}(r) j_\ell(kr)], \quad (9)$$

where j_ℓ are spherical Bessel functions, while δ_m is the dark-matter over-density, related to galaxy overdensity via the bias factor $b(r)$. The corresponding contribution from galaxy overdensities (retaining only the dominant clustering contribution) reads

$$\Delta_\ell(k) = \int dr W(r) [b(r) \delta_{m,k}(r) j_\ell(kr)], \quad (10)$$

where $W(r)$ is a window function normalized to one which selects the redshift bin in the galaxy catalog we want to consider in the cross-correlations.

The framework presented so far is general and can be applied to any astrophysical background component across any frequency band. We will now focus on the specific case of PTAs, where the sources are binary systems of massive black holes residing in galaxies. In the next section, we will estimate the contribution of shot noise in this context, both for the auto-correlation spectrum and for the cross-correlation with the galaxy distribution.

B. Shot noise

Our goal is to demonstrate from first principles that if the source distribution is a sub-sample of the underlying galaxy distribution, cross-correlations are less affected by shot noise than auto-correlations. We will also derive explicit expressions for both contributions.

1. Compound statistics

When counting the number of massive BBH, we have two levels of stochasticity: one galaxy may or may not contain a black hole binary, and the distribution of galaxies is stochastic and modeled as Poisson-distributed. We write the number of black hole binaries as

$$N_{\text{BBH}} = \sum_{i=1}^{N_G} X_i, \quad (11)$$

where X_i follows a binomial distribution $X_i \sim B(1, \beta_X)$, hence $\langle X_i \rangle = \beta_X$ and $\text{Var}(X_i) = \beta_X(1 - \beta_X)$. In practice $\beta_X \ll 1$, so that most galaxies do not contain a binary emitting in the relevant frequency band.

Using properties of compound statistics derived in Appendix A and recalling that the covariance of two variables Y and Z is defined as $\text{Var}(Y, Z) = \langle YZ \rangle - \langle Y \rangle \langle Z \rangle$, one finds

$$\langle N_{\text{BBH}} \rangle = \beta_X \langle N_G \rangle, \quad (12a)$$

$$\text{Var}(N_{\text{BBH}}) = \beta_X \langle N_G \rangle, \quad (12b)$$

$$\text{Var}(N_{\text{BBH}}, N_G) = \beta_X \langle N_G \rangle. \quad (12c)$$

We observe that N_{BBH} is also a Poissonian variable.

2. A heuristic derivation

Let us try to have an intuition of why cross-correlating the stochastic background map to a galaxy map helps with the shot noise problem. To present a heuristic derivation, we simplify our treatment and notation: we fix a frequency bin, we consider a set of radial bins and we assume that all sources have the same luminosity L . Recalling that only objects in the same distance bin correlate, we can schematically write

$$\Omega_{\text{GW}} = \sum_r \Omega_{\text{GW}}(r) = \sum_r N_{\text{BBH}}(r) \frac{L}{\rho_c 4\pi r^2}, \quad (13)$$

where $L/(4\pi r^2)$ is the energy flux associated to the GW event. For the galaxy distribution, we write

$$N_G = \sum_r N_G(r), \quad (14a)$$

$$\Delta = \sum_r \frac{N_G(r) - \langle N_G \rangle}{\langle N_G \rangle}. \quad (14b)$$

Then using results from previous section, one has

$$\text{Var}(\Delta) = \frac{1}{\langle N_G \rangle^2} \sum_r \text{Var}(N_G(r)) = \frac{1}{\langle N_G \rangle}, \quad (15a)$$

$$\begin{aligned} \text{Var}(\Omega_{\text{GW}}) &= \sum_r \left(\frac{L}{\rho_c 4\pi r^2} \right)^2 \text{Var}(N_{\text{BBH}}(r)) \\ &= \sum_r \frac{\langle \Omega_{\text{GW}}(r) \rangle^2}{\langle N_{\text{BBH}}(r) \rangle}, \end{aligned} \quad (15b)$$

$$\begin{aligned} \text{Var}(\Omega_{\text{GW}}, \Delta) &= \frac{1}{\langle N_G \rangle} \sum_r \frac{L}{\rho_c 4\pi r^2} \text{Var}(N_{\text{BBH}}(r), N_G(r)) \\ &= \frac{\langle \Omega_{\text{GW}} \rangle}{\langle N_G \rangle}. \end{aligned} \quad (15c)$$

Note that $\text{Var}(\Omega_{\text{GW}})$ is suppressed by the number of massive black hole binaries (at fixed Ω_{GW}). Since $\langle N_G \rangle \ll \langle N_{\text{BBH}} \rangle$ (for $\beta_X \ll 1$), the relative cross-correlation variance is expected to be smaller than the auto-correlation.

3. A more formal derivation of shot noise

Let us refine the derivation above, giving up the assumption that sources have all the same luminosity. We consider a binned catalog of sources (in our case massive black holes in binaries) and look at their correlation function. Define $\Delta_{i,f,\mathcal{M}}$ to be the source overdensity in a spatial bin i , frequency bin f , and chirp mass bin \mathcal{M} . The two point function of this observable $\langle \Delta_{i,f,\mathcal{M}} \Delta_{j,f',\mathcal{M}'} \rangle$ is given by two terms

$$\langle \Delta_{i,f,\mathcal{M}} \Delta_{j,f',\mathcal{M}'} \rangle = \frac{1}{V_c \Delta \log f \Delta \log \mathcal{M} a^3 \bar{n}_s} \delta_{ff'} \delta_{\mathcal{M}\mathcal{M}'} \delta_{ij} + \xi_{ij}^s, \quad (16)$$

where ξ_{ij}^s is the binned correlation function of the underlying, smooth, density field, δ_s , and $V_c \Delta \log f \Delta \log \mathcal{M} a^3 \bar{n}_s$ is the mean number of sources in a spatial pixel of comoving volume V_c , frequency pixel of volume $\Delta \log f$, and chirp mass pixel

$\Delta \log \mathcal{M}$. Finally, δ_{ij} is the Kronecker symbol which arises from the Poisson sampling of the underlying, smooth density field, while the Kronecker in frequency and chirp mass space comes from the fact that only sources emitting at the same frequency are correlated. If we take the continuous limit of a binned survey, we find

$$\begin{aligned} \Delta_{i,f,\mathcal{M}} &\rightarrow \delta_s(\mathbf{x}, \log f, \log \mathcal{M}), \\ \delta_{ij} &\rightarrow V_c \delta^{(3)}(\mathbf{x} - \mathbf{x}'), \\ \delta_{ff'} &\rightarrow \Delta \log f \delta(\log f - \log f'), \\ \delta_{\mathcal{M}\mathcal{M}'} &\rightarrow \Delta \log \mathcal{M} \delta(\log \mathcal{M} - \log \mathcal{M}'). \end{aligned} \quad (17)$$

It is convenient to split the observed source overdensity into a smooth clustering part $\delta_s(\mathbf{x}, \log f, \log \mathcal{M})$ and Poissonian contribution

$$\hat{\delta}_s = \delta_s(\mathbf{x}, \log f, \log \mathcal{M}) + \delta_s^{\text{shot}}(\mathbf{x}, \log f, \log \mathcal{M}), \quad (18)$$

where with a hat we denote observable quantities and the arguments on the left hand side are understood for shortness. The first contribution on the right hand side is due to clustering while for the Poissonian contribution one has

$$\begin{aligned} &\left\langle \delta_s^{\text{shot}}(\mathbf{x}, \log f, \log \mathcal{M}) \delta_s^{\text{shot}}(\mathbf{x}', \log f', \log \mathcal{M}') \right\rangle \\ &= \frac{1}{a^3 \bar{n}_s} \delta^{(3)}(\mathbf{x} - \mathbf{x}') \delta(\log f - \log f') \delta(\log \mathcal{M} - \log \mathcal{M}'), \end{aligned} \quad (19)$$

where the quantity at the denominator $n_s = n_s(z, \log f, \log \mathcal{M})$ is the density of binaries per units $\log f$ and $\log \mathcal{M}$. We use this result to compute the correlation function of the background anisotropies accounting for both clustering and Poissonian components. We assume in first approximation that the clustering of sources follows the clustering of galaxies i.e. $\delta_s(\mathbf{x}, \log f, \log \mathcal{M}) = \delta_G(\mathbf{x})$.¹ We get

$$\begin{aligned} \langle \delta \hat{\Omega}_{\text{GW}}(\mathbf{n}) \delta \hat{\Omega}_{\text{GW}}(\mathbf{n}') \rangle &= \frac{1}{(4\pi)^2} \int dr \int d \log f \int d \log \mathcal{M} \frac{\partial \bar{\Omega}_{\text{GW}}}{\partial r \partial \log \mathcal{M}} \int dr' \int d \log f' \int d \log \mathcal{M}' \frac{\partial \bar{\Omega}_{\text{GW}}}{\partial r' \partial \log \mathcal{M}'} \\ &\times \left[\langle \delta_G(\mathbf{x} = \mathbf{n}r) \delta_G(\mathbf{x}' = \mathbf{n}'r') \rangle + \delta^{(3)}(\mathbf{x} - \mathbf{x}') \delta(\log f - \log f') \delta(\log \mathcal{M} - \log \mathcal{M}') \frac{1}{a^3 \bar{n}_s} \right], \end{aligned} \quad (20)$$

where we made use of (3d) and (C10). Expanding in terms of spherical harmonics

$$\delta \hat{\Omega}_{\text{GW}}(\mathbf{n}) = \sum_{\ell m} \hat{a}_{\ell m} Y_{\ell m}(\mathbf{n}), \quad (21)$$

and using

$$\delta^{(3)}(\mathbf{x} - \mathbf{x}') = \frac{\delta(r - r')}{r^2} \sum_{\ell m} Y_{\ell m}(\mathbf{n}) Y_{\ell m}^*(\mathbf{n}'), \quad (22)$$

¹ Notice that this is just an approximation and a more refined model should e.g. consider that in fact massive galaxies are more likely to host black holes in binaries [46]. However this would not change the result for shot noise, whose computation is the main goal of our treatment.

we find that

$$\langle \hat{a}_{\ell m} \hat{a}_{\ell' m'}^* \rangle = \langle a_{\ell m} a_{\ell' m'}^* \rangle + \delta_{m m'} \delta_{\ell \ell'} \times \int \frac{dr}{(4\pi)^2} \int d \log f \int d \log \mathcal{M} \left| \frac{\partial \bar{\Omega}_{\text{GW}}}{\partial r \partial \log \mathcal{M}} \right|^2 \frac{1}{r^2} \frac{1}{a^3 \bar{n}_s}, \quad (23)$$

where the first contribution is the theoretical one, given in eq. (5a) and the second the shot noise component. Using the standard definition

$$\langle \delta \hat{\Omega}_{\ell m} \delta \hat{\Omega}_{\ell' m'}^* \rangle \equiv \hat{C}_\ell \delta_{\ell \ell'} \delta_{m m'}, \quad (24)$$

we immediately find that

$$\hat{C}_\ell = C_\ell^{\text{GW}} + N_{\text{shot}}^{\text{GW}}, \quad (25)$$

where

$$N_{\text{shot}}^{\text{GW}} \equiv \int \frac{dr}{(4\pi)^2} \int d \log f \int d \log \mathcal{M} \left| \frac{\partial \bar{\Omega}_{\text{GW}}}{\partial r \partial \log \mathcal{M}} \right|^2 \frac{1}{r^2} \frac{1}{a^3 \bar{n}_s}. \quad (26)$$

One can repeat the same reasoning for the cross-correlation and the galaxy auto-correlation. Using results of the heuristic argument, we can directly see that

$$N_{\text{shot}}^{\text{GW}\Delta} = \int \frac{dr}{4\pi r^2} \frac{1}{a^3 \bar{n}_G(r)} W(r) \partial_r \bar{\Omega}_{\text{GW}}(r), \quad (27a)$$

$$N_{\text{shot}}^\Delta = \int \frac{dr}{r^2} \frac{1}{a^3 \bar{n}_G(r)} W^2(r), \quad (27b)$$

which scale as $1/(a^3 \bar{n}_G)$ which is the inverse of the comoving number density of galaxies. In the Appendix D, we explain how the shot noise contribution for the GW auto-correlation can be estimated from a catalog, and we prove the equivalence between the discrete and continuous descriptions.

To conclude: we found that while shot noise of the AGWB energy density auto-correlation scales as the inverse number of sources (black hole binaries), the shot noise of the cross-correlation with the galaxy distribution scales as the inverse number of galaxies, hence shot noise of a cross-correlation map is much more suppressed than shot noise of the AGWB auto-correlation.

III. RESULTS

Before we embark on assessing the impact of cross-correlations on the detectability of the signal, we note that the weight function, $W(r)$, should be chosen so as to maximize the SNR of cross-correlations. This can be done as long as radial information (i.e. accurate redshifts) are available for all galaxies in the survey we cross-correlate with, which we will assume here. As detailed in [37], the optimal weights can be derived in terms of a Wiener filter, leading to the result

$$W(r) \equiv \frac{\partial_r \bar{\Omega}_{\text{GW}}(r)}{\bar{\Omega}_{\text{GW}}}, \quad (28)$$

Physically this means that we approximately weight all galaxies by a $1/r^2$ factor, hence mimicking the properties of a background mapped in intensity.

A. Signal to noise ratio

We can now estimate the signal to noise of the auto-correlation and cross-correlation. We assume that shot noise is the dominant noise component, i.e. we assume an ideal experiment. The signal to noise of the AGWB auto-correlation is given by (see Appendix B for a derivation)

$$\left(\frac{S}{N} \right)_{\text{GW}, \ell}^2 = 2(2\ell + 1) \left(\frac{C_\ell^{\text{GW}}}{C_\ell^{\text{GW}} + N_{\text{shot}}^{\text{GW}}} \right)^2, \quad (29)$$

while the one of the cross-correlation is given by

$$\left(\frac{S}{N} \right)_{\text{GW}\Delta, \ell}^2 = \frac{(2\ell + 1)(C_\ell^{\text{GW}\Delta})^2}{(C_\ell^{\text{GW}\Delta} + N_{\text{shot}}^{\text{GW}\Delta})^2 + (C_\ell^{\text{GW}} + N_{\text{shot}}^{\text{GW}})(C_\ell^\Delta + N_{\text{shot}}^\Delta)}. \quad (30)$$

One can combine the various multipoles to constrain the global amplitude of the angular power spectrum. Then we define a cumulative SNR as

$$\left(\frac{S}{N} \right)_{\text{GW}}^2 = \sum_{\ell}^{\ell_{\text{max}}} \left(\frac{S}{N} \right)_{\text{GW}, \ell}^2, \quad (31)$$

and similarly for the cross-correlation.

In both (29) and (30) the dominant contribution to the denominator is coming from the variance of AGWB auto-correlation $N_{\text{shot}}^{\text{GW}}$, which appears quadratically in (29) and linearly in (30). Hence the SNR of cross-correlation will be typically enhanced with respect to the AGWB auto-correlation one.

B. Astrophysical modeling and numerical results

We make use of the astrophysical BBH populations of [44, 45], and we refer the reader to those papers for full details. In short, the BBH cosmic population is derived from observations of the galaxy mass function $\phi(M_g, z)$ and pair fraction $\mathcal{F}(z, M_g, q_g)$, as a function of galaxy mass M_g , redshift z and mass ratio of galaxy pairs $q_g < 1$. These observables can be combined with a merger time scale $\tau(z, M_g, q_g)$ inferred by numerical detailed simulations to get a galaxy merger rate as:

$$\frac{d^3 n_g}{dz dM_g dq_g} = \frac{\phi(M_g, z)}{M_g \ln 10} \frac{\mathcal{F}(z, M_g, q_g)}{\tau(z, M_g, q_g)} \frac{dt_r}{dz}, \quad (32)$$

where t_r is the rest frame cosmic time and dt_r/dz converts time into redshift for a given cosmology. The BBH merger rate is then computed by populating galaxies with black holes according to observed scaling relations of the form:

$$\log_{10} M_{\text{BH}} = \alpha + \beta \log_{10} X, \quad (33)$$

where X can be the galaxy bulge mass, or its mid-infrared luminosity or velocity dispersion σ (see [44] for a list of those relations).

Here, we take $\phi(M_g, z)$ from [47], $\mathcal{F}(z, M_g, q_g)$ from [48] and $\tau(z, M_g, q_g)$ from [49]. Further, we use the $M - \sigma$ relation given by [50], obtaining a GW background with nominal characteristic strain amplitude at the reference frequency of one year $h_{1\text{yr}} = 2.4 \times 10^{-15}$ where the strain amplitude $h_c(f) = h_{1\text{yr}}(f \times \text{yr})^{-2/3}$ is related to the GW energy density by $\bar{\Omega}_{\text{GW}}(f) = 2\pi^2/3(f/H_0)^2 h_c^2(f)$. Using the value $1/H_0 = 14.4 \times 10^9 \text{ yr}$ one finds $\bar{\Omega}_{\text{GW}}(f = \text{yr}^{-1}) \simeq 8 \times 10^{-9}$, consistent with the one inferred from the EPTA DR2new analysis [3].

Given a BBH merger rate, we compute the cosmic population of inspiraling BBHs, $d^3N/(dz d\mathcal{M} d\ln f)$, by assuming circular-GW driven systems. One can then sample this distribution in the parameter region $(\mathcal{M} > 10^7 M_\odot) \cap (f > 10^{-9} \text{ Hz}) \cap (z < 1.3)$. One sample draw counts $\approx 100\text{K}$ binaries, with chirp masses, redshift and GW emission frequency, that are used to construct the GW background energy density as described in Appendix C.²

Finally, in order to compute the statistical properties of the GW background, we also need to choose how to distribute the GW sources across the sky. We assume that the distribution of galaxies follows the distribution of dark matter halos with bias factor that we assume to be scale-independent and with redshift evolution given by $b(z) = b_0 \sqrt{1+z}$ and $b_0 = 1.5$ [52, 53]. Finally, as mentioned earlier, we assume that the clustering properties of the massive BBH population are identical to those of the underlying galaxy distribution. This is, of course, a simplifying approximation, as we expect more massive galaxies to be more likely to host massive black holes. In other words, the population of massive BBH is expected to be *more clustered* than the galaxy distribution. Since refining this bias model would likely strengthen the clustering signal, our simplifying assumption is conservative for the purposes of this study. We also use a constant comoving galaxy density $a^3 n_G \sim 0.1 \text{ Mpc}^{-3}$.

As already mentioned, we expect the AGWB strain map to be dominated by a few very bright sources: by resolving them, anisotropies of the AGWB generated by the remaining unresolved population are a representative sample of large scale structure anisotropies. We filter out from the background budget sources whose strain is higher than the current EPTA sensitivity curve [54], roughly corresponding to $h_{\text{eff}} > 10^{-14}$ around the sweet spot of the sensitivity curve. We have here introduced an effective strain h_{eff} defined by

$$h_{\text{eff}}^2(f) = h^2(f) f T_{\text{obs}}, \quad (34)$$

where $T_{\text{obs}} = 16 \text{ yr}$ and $h(f) = 8/(\sqrt{10} D_L) G \mathcal{M}_z [\pi G \mathcal{M}_z f]^{2/3}$ with $\mathcal{M}_z = (1+z)\mathcal{M}$ is the polarization and inclination averaged strain (see e.g. [51] with proper factors of redshift accounted for). As the sensitivity of a given PTA observatory

² A Monte-Carlo sampling of the population returns correctly a discrete number of sources, while the semi-analytical result contains spurious contributions from *fractional sources* that are clearly not present [51]. In other words, sampling is needed because when using an analytical formula, one would also need to add a 'fraction of sources,' while Monte Carlo methods avoid this issue.

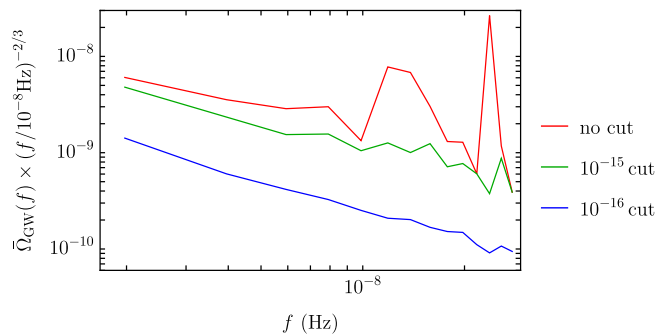


FIG. 1. Background energy density $\bar{\Omega}_{\text{GW}}(f)$ as function of frequency, for the three different cut-off values used in the filtering procedure.

will improve, more and more sources will be detectable individually: when deriving forecasts for future experiments, the filtering should be performed following the iterative procedure of [55], accounting in the computation of the expected noise budget for both a pure noise contribution and contribution of the unresolvable background component.³ Since our goal is just to quantify the effect of filtering without targeting a specific future PTA mission, we test the effect of moving the threshold on h_{eff} , filtering out sources with $h_{\text{eff}} > 10^{-15}$ and with $h_{\text{eff}} > 10^{-16}$, the latter corresponding to the plateau of the SKA sensitivity curve [55].⁴ We refer to these three values for the filtering threshold as "no cut" (as the EPTA sensitivity effectively does not allow to resolve any individual source), "10⁻¹⁵ cut" and "10⁻¹⁶ cut".

In Fig. 1 we show the background energy density as function of frequency, for the three aforementioned cut-off values. In the "no cut" situation, after averaging over modulations, the scaling is roughly $\propto f^{2/3}$ as expected. The bumps in the red curve are due to the contribution of a few very bright sources that dominate the total signal at high frequencies (plotting source contributions individually, they would appear as spikes at a given frequency). We observe that the filtering procedure has the effect of eliminating these high-frequency bumps and changing the low-frequency scaling. Indeed for a given threshold $h_{\text{eff}}^{\text{cut}}$, we infer from (34) that $\mathcal{M}_{\text{max}} \propto (h_{\text{eff}}^{\text{cut}})^{3/5} f^{-7/10}$, hence the larger the frequency, the more sources are removed from the catalog, leaving behind a smaller residual amplitude.

Fig. 2 represents for the three situations the angular power spectrum of auto- and cross-correlations, and the corresponding shot noise contributions.⁵ We see that while the auto-

³ We stress that both these contributions are accounted for when computing the sensitivity curve using real PTA data.

⁴ We stress again that in the context of SKA a proper filtering procedure would need to account not only for the instrumental noise component, but also for the background budget. In this respect, a threshold $h_{\text{eff}} > 10^{-16}$ for filtering out resolvable events with SKA is optimistic.

⁵ Our results for the cross-spectrum are compatible in order of magnitude with those of [56] (Fig. 3), where a different set of astrophysical models is used.

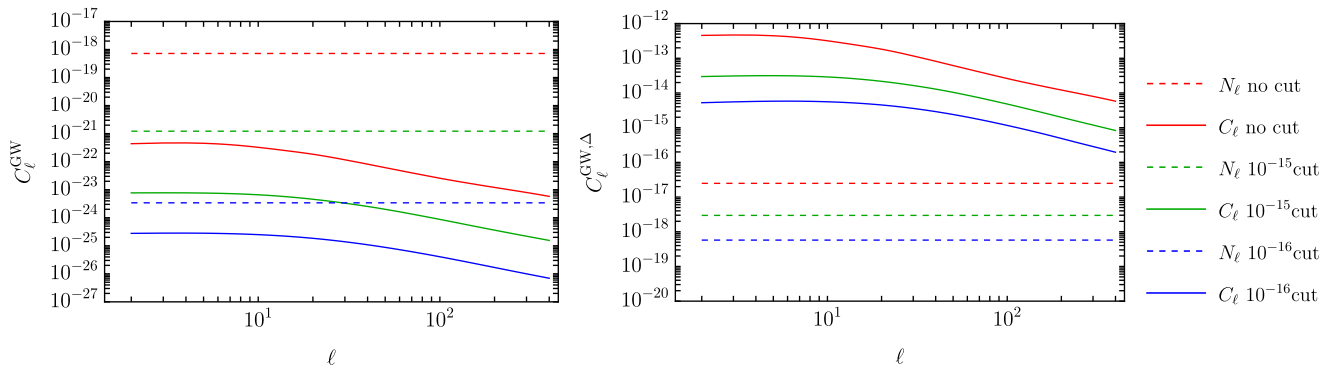


FIG. 2. Angular power spectrum of auto-correlation (left panel) and cross-correlation (right panel) and corresponding shot noise contributions. The signal is integrated over the PTA frequency range.

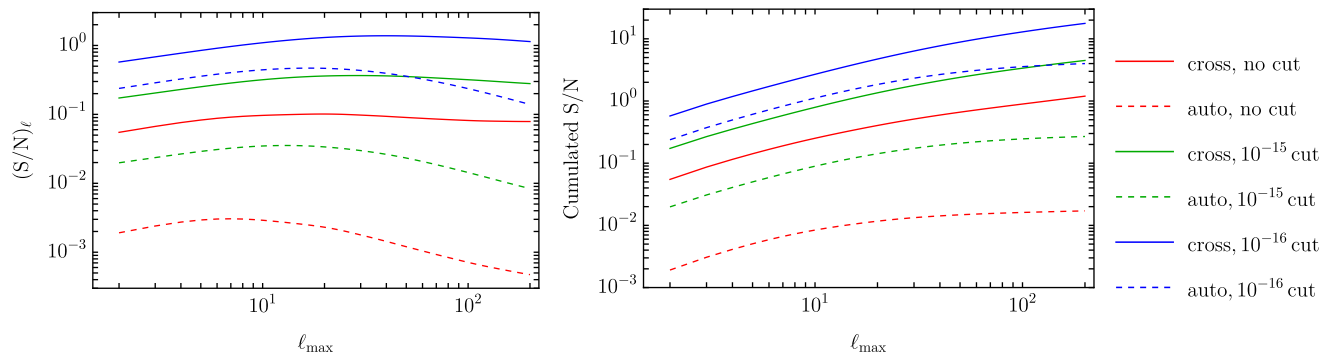


FIG. 3. *Left*: SNR as function of the multipole ℓ of cross-correlation (dashed lines) and of auto-correlation (continuous lines) for an ideal experiment in which the shot noise is the only noise component. *Right*: corresponding cumulative SNR as function of ℓ_{\max} .

correlation map is shot noise dominated ($N_{\text{shot}}^{\text{GW}} \gg C_{\ell}^{\text{GW}}$), the shot noise contribution to the cross-correlation is much suppressed ($N_{\text{shot}}^{\text{GW}\Delta} \ll C_{\ell}^{\text{GW}\Delta}$). We observe that the filtering procedure reduces both the angular power spectrum of the clustering signal and the shot noise component, for both auto- and cross-angular power spectra.

In Fig. 3 (left panel) we show the SNR for auto- and cross-correlations (for the three cut-off values) as a function of the multipole ℓ . On the right panel we show the corresponding cumulative SNR, as a function of ℓ_{\max} . As expected, the SNR of the cross-correlation outperforms the auto-correlation one (by more than two orders of magnitudes in the absence of a cut-off). This is due to the aforementioned hierarchy between signal and noise components along with $N_{\text{shot}}^{\Delta} \ll C_{\ell}^{\Delta}$, i.e. the fact that the auto-correlation SNR scales as $\sqrt{2(2\ell+1)}C_{\ell}^{\text{GW}}/N_{\text{shot}}^{\text{GW}}$ whereas for cross-correlation it scales as $\sqrt{(2\ell+1)}C_{\ell}^{\text{GW}\Delta}/\sqrt{N_{\text{shot}}^{\text{GW}}C_{\ell}^{\Delta}}$.

We observe that even in the ideal case under study where the instrumental noise is set to zero (the noise is just shot noise), the SNR of single multipoles is never much larger than 1, unless a very low threshold of detection of single events is chosen. However, the cumulative SNR is above 1 already at $\ell_{\max} = 4$ (corresponding to ~ 25 pulsars), for a filtering threshold of 10^{-16} , and it is above 1 for $\ell_{\max}=13$ for a thresh-

old of 10^{-15} . This indicates that, while the reconstruction of the shape of the angular power spectrum will be challenging, it will be potentially possible to constrain the global amplitude of the spectrum, by combining the information from different multipoles.

We conclude observing that to obtain these results, we have fixed the value of the comoving galaxy number density equal to $a^3 n_G = 0.1 \text{ Mpc}^{-3}$, however our results for the SNR depend very mildly on this choice. Indeed the SNR of the auto-correlation map does not depend on the galaxy number density assumed, while, for any reasonable value of $a^3 n_G$, the dominant contribution to the noise of the cross-correlation map comes from the $\propto N_{\ell}^{\text{GW}} C_{\ell}^{\Delta}$ contribution in the denominator of eq. (29), which does not depend on the galaxy number density.

IV. DISCUSSION AND CONCLUSIONS

In this article, we explored the shot noise problem in the context of PTA observations, in isolation from other sources of noise. We derived from first principles the expression for the shot noise of the AGWB auto-correlation and the cross-correlation with a dense galaxy map. Using catalogs of massive BBH from [44, 45], we showed that, unlike the auto-correlation, the cross-correlation map is not shot noise

dominated: for an ideal experiment, the SNR of the cross-correlation outperforms the auto-correlation by more than two orders of magnitude. We also tested the effect of a filtering procedure that removes the brightest sources from the total background: this procedure further reduces shot noise, as the brightest sources dominate the background budget, obscuring the contribution of the unresolved population that traces the large-scale structure. A similar result was recently found in [13], relying on numerical simulations. However, while our findings are consistent with the simulation results of [13], our analytic treatment disagrees with the explanation proposed in that reference.⁶ In our derivations, we considered an ideal experiment with zero instrumental noise; however, when filtering out bright sources, we had to assume a threshold value to determine whether a source is resolvable individually. To do so, we considered the current EPTA sensitivity curve (effectively resulting in no resolvable sources), a threshold value corresponding to SKA sensitivity, and an intermediate scenario. We found that the amplitude of the angular power spectrum can potentially be detectable using cross-correlation with the galaxy distribution (integrated in redshift), when making use of a filtering procedure compatible with SKA projected sensitivity, and combining the first multipoles of the angular power spectrum up to $\ell_{\max} = 4$, requiring at least a number of pulsars ~ 25 . With a sensitivity one order of magnitude lower than the projected SKA one, i.e. filtering out sources with $h_{\text{eff}} > 10^{-15}$, the global amplitude of the anisotropies can be detected with $\ell_{\max}=13$ requiring at least ~ 200 pulsars, which is more or less twice the number of pulsars currently monitored by the IPTA collaboration. Our results represent the best-case scenario for the detectability of the AGWB in the presence of spatial shot noise. A future study will be dedicated to deriving more realistic forecasts for future PTA experiments and galaxy surveys such as Euclid, properly factoring in the effects of instrumental noise and realistic filtering procedures.

ACKNOWLEDGEMENT

The work of GC and CP is supported by CNRS. The work of GC and MP has received financial support by the SNSF Ambizione grant *Gravitational wave propagation in the clustered universe*. We thank Camille Bonvin and Nastassia Grimm for interesting discussions at different stages of this work. AS acknowledges financial support by the ERC CoG "B Massive" (Grant Agreement: 818691) and ERC AdG "PINGU" (Grant Agreement: 101142079).

⁶ Through a detailed analytic derivation, we demonstrate that shot noise is, in fact, never fully eliminated in cross-correlation maps, contrary to what is claimed in eq. (7) of [13], which states that the cross-correlation map is shot noise free.

Appendix A: General properties of compound statistics

Let us consider N being a random variable with variance $\langle N^2 \rangle - \langle N \rangle^2$ and mean $\langle N \rangle$. Then for a generic function $f(N)$

$$\langle f(N) \rangle = \int f(N)p(N)dN. \quad (\text{A1})$$

We are interested in the statistics of the compound random variable Y given by

$$Y = \sum_{i=1}^N X_i, \quad (\text{A2})$$

where X_i is either 1 or 0, i.e. it is a binomial variable $X_i \sim B(1, \beta)$. It has a probability $p(Y)$, such that

$$p(Y) = \int p(Y|N)p(N)dN. \quad (\text{A3})$$

The conditional probability $p(Y|N)$ can be found from the fact that it is the sum of N random variables (it is a convolution of probabilities), but we do not need to go to this level of sophistication to get convinced that

$$\langle Y \rangle_N = \int Y p(Y|N)dY = N\langle X \rangle. \quad (\text{A4})$$

The subindex on the left hand side means that is an average at N being fixed. For the second moment one has

$$\langle Y^2 \rangle_N = \int Y^2 p(Y|N)dY = N\langle X^2 \rangle + N(N-1)\langle X \rangle^2, \quad (\text{A5})$$

which is obtained by separation of the X_i^2 and the $X_i X_j$ with $i \neq j$.

We can work out the first moments of Y from $p(Y)$. For a generic function of Y , we have

$$\begin{aligned} \langle f(Y) \rangle &= \int f(Y)p(Y)dY \\ &= \int \int f(Y)p(Y|N)p(N)dNdY \\ &= \int p(N)dN \left(\int f(Y)p(Y|N)dY \right) \\ &= \int \langle f(Y) \rangle_N p(N)dN, \end{aligned} \quad (\text{A6})$$

where in the last line the remaining randomness of N has to be treated. The average $\langle Y \rangle$ can be easily computed

$$\langle Y \rangle = \int \langle Y \rangle_N p(N)dN = \int \langle X \rangle N p(N)dN = \langle N \rangle \langle X \rangle. \quad (\text{A7})$$

Similarly for the second moment

$$\begin{aligned} \langle Y^2 \rangle &= \int \langle Y^2 \rangle_N p(N)dN \\ &= \int (N\langle X^2 \rangle + N(N-1)\langle X \rangle^2) p(N)dN \\ &= \langle N \rangle (\langle X^2 \rangle - \langle X \rangle^2) + \langle N^2 \rangle \langle X \rangle^2. \end{aligned} \quad (\text{A8})$$

Hence we obtain the variance of Y

$$\begin{aligned}\langle Y^2 \rangle - \langle Y \rangle^2 &= \langle N \rangle (\langle X^2 \rangle - \langle X \rangle^2) + (\langle N^2 \rangle - \langle N \rangle^2) \langle X \rangle^2 \\ &= \langle N \rangle \langle X^2 \rangle,\end{aligned}\quad (\text{A9})$$

where the last equality holds when N is a Poisson variable. This derivation is valid whatever the statistics for X , and $\langle X^2 \rangle = \langle X \rangle$ if $X \sim B(1, \beta)$. Following the same kind of reasoning we can also get cross correlations between Y and N , and

$$\begin{aligned}\langle YN \rangle &= \int \langle Y \rangle_N N p(N) dN \\ &= \int \langle X \rangle N^2 p(N) dN \\ &= \langle X \rangle \langle N^2 \rangle \\ &= \langle X \rangle (\langle N \rangle + \langle N \rangle^2),\end{aligned}\quad (\text{A10})$$

where the last equality holds when N is Poisson variable. Then

$$\langle YN \rangle - \langle Y \rangle \langle N \rangle = \langle X \rangle \text{Var}(N) = \langle X \rangle \langle N \rangle,\quad (\text{A11})$$

where the last equality holds when N is a Poisson variable.

Appendix B: Signal to noise derivation

Let us assume that our observables are the angular power spectra of the AGWB and galaxy auto-correlations and their cross-correlation angular spectrum, i.e. C_ℓ^{GW} , C_ℓ^Δ and $C_\ell^{\text{GW}\Delta}$ are the observables. The estimator (full sky) of the angular power spectrum is

$$\hat{C}_\ell^{ab} = \frac{1}{2\ell+1} \sum_m a_{\ell m}^a (a_{\ell m}^b)^*,\quad (\text{B1})$$

where $a_{\ell m}^{a,b}$ are Gaussian maps and the indices are defined as $a = (\text{GW}, \Delta)$ and $b = (\text{GW}, \Delta)$. We compute the covariance of this estimator. To make the notation compact, we introduce $X = (C_{\ell_{\min}}^{\text{GW}}, C_{\ell_{\min}}^\Delta, C_{\ell_{\min}}^{\text{GW}\Delta}, \dots, C_{\ell_{\max}}^{\text{GW}}, C_{\ell_{\max}}^\Delta, C_{\ell_{\max}}^{\text{GW}\Delta})$. Then the associated covariance matrix is block diagonal

$$C = \begin{pmatrix} B_{\ell_{\min}} & & 0 \\ & \dots & \\ 0 & & B_{\ell_{\max}} \end{pmatrix},$$

with 3×3 blocks

$$B_\ell = \frac{1}{2\ell+1} \times \begin{pmatrix} 2(C_\ell^{\text{GW}})^2 & 2(C_\ell^{\text{GW}\Delta})^2 & 2(C_\ell^{\text{GW}})(C_\ell^{\text{GW}\Delta}) \\ 2(C_\ell^{\text{GW}\Delta})^2 & 2(C_\ell^\Delta)^2 & 2(C_\ell^\Delta)(C_\ell^{\text{GW}\Delta}) \\ 2(C_\ell^{\text{GW}})(C_\ell^{\text{GW}\Delta}) & 2(C_\ell^\Delta)(C_\ell^{\text{GW}\Delta}) & C_\ell^{\text{GW}} C_\ell^\Delta + (C_\ell^{\text{GW}\Delta})^2 \end{pmatrix},$$

where it is understood that each entry includes a noise part, i.e. one has to replace $C_\ell^{ab} \rightarrow C_\ell^{ab} + N_{\text{shot}}^{ab}$. We have all the ingredients to compute the (non-Gaussian) likelihood of the angular

power spectra X and compute the corresponding Fisher matrix deriving it with respect to the parameters θ_a . The Fisher matrix is defined as

$$F_{ab} = \left\langle -\frac{\partial^2 \ln \mathcal{L}}{\partial \theta_a \partial \theta_b} \right\rangle,\quad (\text{B2})$$

where θ_a are a set of parameters of the model. It is possible to show that only the Gaussian part of the likelihood enters the Fisher matrix. We want to estimate the signal to noise of the galaxy map, hence we parametrize

$$X_\ell = (\mathcal{C}^2 C_\ell^{\text{GW}} + N_{\text{shot}}^{\text{GW}}, C_\ell^\Delta + N_{\text{shot}}^\Delta, \mathcal{C} C_\ell^{\text{GW}\Delta} + N_{\text{shot}}^{\text{GW}\Delta}),\quad (\text{B3})$$

where \mathcal{C} is a book keeping parameter for the amplitude. Then

$$(F_{\mathcal{C}})_\ell = \left(\frac{S}{N} \right)_\ell^2 = (\partial_{\mathcal{C}} X_\ell) \cdot B_\ell^{-1} \cdot (\partial_{\mathcal{C}} X_\ell),\quad (\text{B4})$$

evaluated in $\mathcal{C} = 1$. If we use only the information from the auto-correlation, we get (29) while using only cross-correlation we obtain (30).

Appendix C: The GW energy density

Let us introduce some basic quantities that we extract from the catalog. The chirp mass of a source \mathcal{M} is given by

$$\mathcal{M} = \frac{(m_1 m_2)^{3/5}}{(m_1 + m_2)^{1/5}},\quad (\text{C1})$$

with $m_{1,2}$ the masses of the two black holes in the binary. We focus on the case of an inspiraling BBH, for which the emitted power is given by [57]

$$\frac{dE_s}{dt_s} = \frac{32}{5Gc^5} (\pi G \mathcal{M} f_s)^{10/3} = \frac{32}{5Gc^5} (\pi G \mathcal{M} (1+z)f)^{10/3},\quad (\text{C2})$$

where E_s is the source-frame energy of one source with mass \mathcal{M} and (source-frame) frequency f_s , and t_s is the local cosmic time at the source. The source-frame frequency f_s is related to the observed frequency by $f = f_s/(1+z)$. The observed power is found using $E_o = E_s/(1+z)$ and $dt_o = dt_s(1+z)$, hence

$$\frac{dE_o}{dt_o} = \frac{1}{(1+z)^2} \frac{dE_s}{dt_s}.\quad (\text{C3})$$

We denote the (comoving) number of sources per comoving volume dV_c , per frequency df and per logarithmic chirp mass $d \log \mathcal{M}$ by

$$a^3 n_s(\mathbf{n}, z, \mathcal{M}, f) \equiv f \frac{dN_s}{dV_c d \log(\mathcal{M}) df} \propto f^{-8/3},\quad (\text{C4})$$

where N_s is the number of sources. The previous scaling in frequency is found using that the number of sources in a given frequency band is proportional to the time spent in that band,

along with $d \log f / dt \propto f^{8/3}$. We split this quantity into an angle-averaged term \bar{n}_s , and an anisotropic contribution

$$n_s(\mathbf{n}, z, \mathcal{M}, f) = \bar{n}_s(z, \mathcal{M}, f) + \delta n_s(\mathbf{n}, z, \mathcal{M}, f). \quad (\text{C5})$$

To consider the contributions of the different directions \mathbf{n} to the total energy density parameter at the observer, we then analogously split Ω_{GW} in an angle-averaged term $\bar{\Omega}_{\text{GW}}$ and an anisotropic fluctuation, with the definition (1). The isotropic part is obtained by summing all contributions as in (2a) with

$$\partial_r \bar{\Omega}_{\text{GW}}(f, r) = \frac{f \mathcal{A}(f, r)}{\rho_c} = \int d \log \mathcal{M} \frac{\partial \bar{\Omega}_{\text{GW}}(f, r, \mathcal{M})}{\partial r \partial \log \mathcal{M}}, \quad (\text{C6})$$

where

$$\frac{\partial \bar{\Omega}_{\text{GW}}(f, r, \mathcal{M})}{\partial r \partial \log \mathcal{M}} = \frac{1}{\rho_c} \frac{1}{(1+z)^2} \frac{dE_s}{dt_s} a^3 \bar{n}_s(z, \mathcal{M}, f), \quad (\text{C7})$$

and the function $z = z(r)$ must be used to relate a given redshift z to the conformal distance r .

Denoting the fractional fluctuation in the number density of sources by

$$\delta_s(\mathbf{n}, z, \mathcal{M}) = \frac{\delta n_s(\mathbf{n}, z, \mathcal{M}, f)}{\bar{n}_s(z, \mathcal{M}, f)}, \quad (\text{C8})$$

and using that the GW sources are biased tracers of the underlying distribution of galaxies,

$$\delta_s(\mathbf{n}, z, \mathcal{M}) = b_s(z, \mathcal{M}) \delta_g(\mathbf{n}, z), \quad (\text{C9})$$

we obtain

$$\begin{aligned} \delta \Omega_{\text{GW}}(f, \mathbf{n}) &= \frac{1}{4\pi} \int dr \int d \log \mathcal{M} \\ &\times \frac{\partial \bar{\Omega}_{\text{GW}}(f, r, \mathcal{M})}{\partial r \partial \log \mathcal{M}} b_s(z, \mathcal{M}) \delta_g(\mathbf{n}, z), \end{aligned} \quad (\text{C10})$$

where the integration on the conformal distance r can be replaced by an integral on redshifts using the background cosmology and $dr = dz/H(z)$.

Eq.(C10) relates the anisotropies in the energy density of an astrophysical SGWB to the anisotropies of the large-scale structure where SGWB sources are found. We assume that GW sources follow the same clustering structure as the galaxies, hence we take $b_s = 1$ in our analysis.

Appendix D: Energy density and shot noise from a catalogue

For a given source i , we introduce the following quantity $P_i \equiv (dE_o/dt_o)_i / \rho_c = (dE_s/dt_s)_i / \rho_c / (1+z_i)^2$, such that for a collection of N sources in directions \mathbf{n}_i

$$\Omega_{\text{GW}}(\mathbf{n}) = \sum_{i=1}^N \left(\frac{P_i}{4\pi r_i^2} \right) \delta^2(\mathbf{n}, \mathbf{n}_i). \quad (\text{D1})$$

Using

$$\delta^2(\mathbf{n}_1, \mathbf{n}_2) = \sum_{\ell m} Y_{\ell m}(\mathbf{n}_1) Y_{\ell m}^*(\mathbf{n}_2), \quad (\text{D2})$$

and an expansion $\Omega_{\text{GW}}(\mathbf{n}) = \sum_{\ell m} \Omega_{\ell m}^{\text{GW}} Y_{\ell m}(\mathbf{n})$ we get

$$\Omega_{\ell m}^{\text{GW}} = \sum_{i=1}^N \left(\frac{P_i}{4\pi r_i^2} \right) Y_{\ell m}^*(\mathbf{n}_i). \quad (\text{D3})$$

An estimator of the C_ℓ^{GW} defined in (5a) is

$$\hat{C}_\ell^{\text{GW}} = \frac{1}{2\ell+1} \sum_{m=-\ell}^{\ell} \Omega_{\ell m}^{\text{GW}} \Omega_{\ell m}^{\text{GW}*}, \quad (\text{D4})$$

and for random positions of the sources, that is sources which are not located according to clustering properties, it is non-vanishing only due to the Poissonian nature of the source distribution. We want to average this estimator over the direction realizations of the sources, that is over random realizations of the set of directions $\{\mathbf{n}_i\}$, so as to estimate the shot noise. We shall use that (see e.g. [58] or appendix D of [27])

$$\langle Y_{\ell m}(\mathbf{n}_{i_1}) \rangle_{\{\mathbf{n}_i\}} = \frac{\delta_\ell^0 \delta_m^0}{\sqrt{4\pi}}, \quad (\text{D5})$$

and for $(\ell, m) \neq (0, 0)$

$$\langle Y_{\ell m}(\mathbf{n}_{i_1}) Y_{\ell' m'}^*(\mathbf{n}_{i_1}) \rangle_{\{\mathbf{n}_i\}} = \frac{\delta_{\ell\ell'} \delta_{mm'}}{4\pi}. \quad (\text{D6})$$

Then when averaging over all random positions of these N sources

$$4\pi \langle \Omega_{\text{GW}}(\mathbf{n}) \rangle_{\{\mathbf{n}_i\}} = \sqrt{4\pi} \langle \Omega_{00}^{\text{GW}} \rangle_{\{\mathbf{n}_i\}} = \sum_{i=1}^N \frac{P_i}{4\pi r_i^2}, \quad (\text{D7})$$

$$\langle \hat{C}_\ell^{\text{GW}} \rangle_{\{\mathbf{n}_i\}} = \frac{1}{4\pi} \sum_{i=1}^N \left(\frac{P_i}{4\pi r_i^2} \right)^2. \quad (\text{D8})$$

We identify the average GW density as $\bar{\Omega}_{\text{GW}} = 4\pi \langle \Omega_{\text{GW}}(\mathbf{n}) \rangle_{\{\mathbf{n}_i\}}$ and shot noise with $N_{\text{shot}}^{\text{GW}} = \langle \hat{C}_\ell^{\text{GW}} \rangle_{\{\mathbf{n}_i\}}$.

In order to check the consistency with the continuous integral formulas we use

$$\sum_{i=1}^N \rightarrow \int d \log f \int d \log \mathcal{M} \int dr (4\pi r^2 a^3 \bar{n}_s), \quad (\text{D9})$$

and indeed applying this replacement rule to (D7) we get (C7). Also for shot noise we get

$$\langle \hat{C}_\ell^{\text{GW}} \rangle_{\{\mathbf{n}_i\}} \simeq \int d \log f \int d \log \mathcal{M} \int dr a^3 \bar{n}_s r^2 \left(\frac{P}{4\pi r^2} \right)^2 \quad (\text{D10})$$

$$\simeq \int d \log f \int d \log \mathcal{M} \int dr \frac{a^3 \bar{n}_s}{(4\pi)^2 r^2} \left(\frac{dE_s/dt_s}{(1+z)^2 \rho_c} \right)^2,$$

and using (C7) we recover (26). Hence when using a catalog, we have to use (D7) to estimate the background GW density, and (D8) to estimate the shot noise.

- [1] G. Agazie *et al.* (NANOGrav), *Astrophys. J. Lett.* **951**, L8 (2023), arXiv:2306.16213 [astro-ph.HE].
- [2] D. J. Reardon *et al.*, *Astrophys. J. Lett.* **951**, L6 (2023), arXiv:2306.16215 [astro-ph.HE].
- [3] J. Antoniadis, P. Arumugam, S. Arumugam, S. Babak, M. Bagchi, A.-S. Bak Nielsen, C. G. Bassa, A. Bathula, A. Berthureau, M. Bonetti, E. Bortolas, P. R. Brook, M. Burgay, R. N. Caballero, A. Chalumeau, D. J. Champion, S. Chantlaridis, S. Chen, I. Cognard, S. Dandapat, D. Deb, S. Desai, G. Desvignes, N. Dhanda-Batra, C. Dwivedi, M. Falxa, R. D. Ferdman, A. Franchini, J. R. Gair, B. Goncharov, A. Gopakumar, E. Graikou, J.-M. Grießmeier, L. Guillemot, Y. J. Guo, Y. Gupta, S. Hisano, H. Hu, F. Iraci, D. Izquierdo-Villalba, J. Jang, J. Jawor, G. H. Janssen, A. Jessner, B. C. Joshi, F. Kareem, R. Karuppusamy, E. F. Keane, M. J. Keith, D. Kharbanda, T. Kikunaga, N. Kolhe, M. Kramer, M. A. Krishnakumar, K. Lackeos, K. J. Lee, K. Liu, Y. Liu, A. G. Lyne, J. W. McKee, Y. Maan, R. A. Main, M. B. Mickaliger, I. C. Njũ, K. Nobleson, A. K. Paladi, A. Parthasarathy, B. B. P. Perera, D. Perrodin, A. Petiteau, N. K. Porayko, A. Possenti, T. Prabu, H. Quelquejay Leclere, P. Rana, A. Samajdar, S. A. Sanidas, A. Sesana, G. Shaifullah, J. Singha, L. Speri, R. Spiewak, A. Srivastava, B. W. Stappers, M. Surnis, S. C. Susarla, A. Subobhanan, K. Takahashi, P. Tarafdar, G. Theureau, C. Tiburzi, E. van der Wateren, A. Vecchio, V. Venkatraman Krishnan, J. P. W. Verbiest, J. Wang, L. Wang, and Z. Wu, *A50* (2023).
- [4] H. Xu *et al.*, *Res. Astron. Astrophys.* **23**, 075024 (2023), arXiv:2306.16216 [astro-ph.HE].
- [5] J. D. Romano and N. J. Cornish, (2016), arXiv:1608.06889 [gr-qc].
- [6] F. A. Jenet and J. D. Romano, *Am. J. Phys.* **83**, 635 (2015), arXiv:1412.1142 [gr-qc].
- [7] J. D. Romano and B. Allen, (2023), arXiv:2308.05847 [gr-qc].
- [8] N. Grimm, M. Pijnenburg, G. Cusin, and C. Bonvin, (2024), arXiv:2411.08744 [gr-qc].
- [9] N. Grimm, M. Pijnenburg, G. Cusin, and C. Bonvin, (2024), arXiv:2404.05670 [astro-ph.CO].
- [10] M. Anholm, S. Ballmer, J. D. E. Creighton, L. R. Price, and X. Siemens, *Phys. Rev. D* **79**, 084030 (2009), arXiv:0809.0701 [gr-qc].
- [11] C. M. F. Mingarelli, T. Sidery, I. Mandel, and A. Vecchio, *Phys. Rev. D* **88**, 062005 (2013), arXiv:1306.5394 [astro-ph.HE].
- [12] P. F. Depta, V. Domcke, G. Franciolini, and M. Pironi, (2024), arXiv:2407.14460 [astro-ph.CO].
- [13] F. Semenzato, J. A. Casey-Clyde, C. M. F. Mingarelli, A. Raccañelli, N. Bellomo, N. Bartolo, and D. Bertacca, (2024), arXiv:2411.00532 [astro-ph.CO].
- [14] R. C. Bernardo, G.-C. Liu, and K.-W. Ng, *JCAP* **04**, 034 (2024), arXiv:2312.03383 [gr-qc].
- [15] G. Cusin, R. Durrer, and P. G. Ferreira, *Phys. Rev. D* **99**, 023534 (2019), arXiv:1807.10620 [astro-ph.CO].
- [16] K. Grunthal *et al.*, (2024), 10.1093/mnras/stae2573, arXiv:2412.01214 [astro-ph.HE].
- [17] G. Agazie *et al.*, (2024), arXiv:2411.13472 [astro-ph.HE].
- [18] J. Gair, J. D. Romano, S. Taylor, and C. M. F. Mingarelli, *Phys. Rev. D* **90**, 082001 (2014), arXiv:1406.4664 [gr-qc].
- [19] E. Roebber and G. Holder, *Astrophys. J.* **835**, 21 (2017), arXiv:1609.06758 [astro-ph.CO].
- [20] W. Qin, K. K. Boddy, M. Kamionkowski, and L. Dai, *Phys. Rev. D* **99**, 063002 (2019), arXiv:1810.02369 [astro-ph.CO].
- [21] S. C. Hotinli, M. Kamionkowski, and A. H. Jaffe, *Open J. Astrophys.* **2**, 8 (2019), arXiv:1904.05348 [astro-ph.CO].
- [22] J. Nay, K. K. Boddy, T. L. Smith, and C. M. F. Mingarelli, *Phys. Rev. D* **110**, 044062 (2024), arXiv:2306.06168 [gr-qc].
- [23] R. C. Bernardo and K.-W. Ng, *JCAP* **11**, 046 (2022), arXiv:2209.14834 [gr-qc].
- [24] R. C. Bernardo and K.-W. Ng, *Phys. Rev. D* **107**, 044007 (2023), arXiv:2208.12538 [gr-qc].
- [25] B. Allen, (2024), arXiv:2404.05677 [gr-qc].
- [26] R. C. Bernardo and K.-W. Ng, (2024), arXiv:2409.07955 [astro-ph.CO].
- [27] C. Pitrou and G. Cusin, (2024), arXiv:2412.12073 [gr-qc].
- [28] X. Siemens, J. Ellis, F. Jenet, and J. D. Romano, *Class. Quant. Grav.* **30**, 224015 (2013), arXiv:1305.3196 [astro-ph.IM].
- [29] N. Pol, S. R. Taylor, and J. D. Romano, *Astrophys. J.* **940**, 173 (2022), arXiv:2206.09936 [astro-ph.HE].
- [30] G. Agazie *et al.* (NANOGrav), *Astrophys. J. Lett.* **956**, L3 (2023), arXiv:2306.16221 [astro-ph.HE].
- [31] M. Rajagopal and R. W. Romani, *Astrophys. J.* **446**, 543 (1995), arXiv:astro-ph/9412038 [astro-ph].
- [32] A. H. Jaffe and D. C. Backer, *Astrophys. J.* **583**, 616 (2003), arXiv:astro-ph/0210148 [astro-ph].
- [33] A. Sesana, A. Vecchio, and C. N. Colacino, *MNRAS* **390**, 192 (2008), arXiv:0804.4476.
- [34] M. Falxa, H. Q. Leclere, and A. Sesana, *Phys. Rev. D* **111**, 023047 (2025), arXiv:2412.01899 [gr-qc].
- [35] A. C. Jenkins and M. Sakellariadou, (2019), arXiv:1902.07719 [astro-ph.CO].
- [36] A. C. Jenkins, J. D. Romano, and M. Sakellariadou, *Phys. Rev. D* **100**, 083501 (2019).
- [37] D. Alonso, G. Cusin, P. G. Ferreira, and C. Pitrou, *Phys. Rev. D* **102**, 023002 (2020), arXiv:2002.02888 [astro-ph.CO].
- [38] G. Cusin, I. Dvorkin, C. Pitrou, and J.-P. Uzan, *Phys. Rev. D* **100**, 063004 (2019), arXiv:1904.07797 [astro-ph.CO].
- [39] K. Z. Yang, J. Suresh, G. Cusin, S. Banagiri, N. Feist, V. Mandic, C. Scarlata, and I. Michaloliakos, *Phys. Rev. D* **108**, 043025 (2023), arXiv:2304.07621 [gr-qc].
- [40] D. Alonso, M. Nikjoo, A. I. Renzini, E. Bellini, and P. G. Ferreira, *Phys. Rev. D* **110**, 103544 (2024), arXiv:2406.19488 [astro-ph.CO].
- [41] G. Cusin, C. Pitrou, and J.-P. Uzan, *Phys. Rev. D* **97**, 123527 (2018), arXiv:1711.11345 [astro-ph.CO].
- [42] G. Cusin, C. Pitrou, and J.-P. Uzan, *Phys. Rev. D* **96**, 103019 (2017), arXiv:1704.06184 [astro-ph.CO].
- [43] C. Pitrou, G. Cusin, and J.-P. Uzan, *Phys. Rev. D* **101**, 081301 (2020), arXiv:1910.04645 [astro-ph.CO].
- [44] A. Sesana, *MNRAS* **433**, L1 (2013), arXiv:1211.5375 [astro-ph.CO].
- [45] P. A. Rosado, A. Sesana, and J. Gair, *Mon. Not. Roy. Astron. Soc.* **451**, 2417 (2015), arXiv:1503.04803 [astro-ph.HE].
- [46] P. A. Rosado and A. Sesana, *MNRAS* **439**, 3986 (2014), arXiv:1311.0883 [astro-ph.CO].
- [47] A. Muzzin, D. Marchesini, M. Stefanon, M. Franx, H. J. McCracken, B. Milvang-Jensen, J. S. Dunlop, J. P. U. Fynbo, G. Brammer, I. Labbé, and P. G. van Dokkum, *Astrophys. J.* **777**, 18 (2013), arXiv:1303.4409 [astro-ph.CO].
- [48] L. de Ravel, O. Le Fèvre, L. Tresse, D. Bottini, B. Garilli, V. Le Brun, D. Maccagni, R. Scaramella, M. Scodeggio, G. Vettolani, A. Zanichelli, C. Adami, S. Arnouts, S. Bardelli, M. Bolzonella, A. Cappi, S. Charlot, P. Ciliegi, T. Contini, S. Foucaud, P. Franzetti, I. Gavignaud, L. Guzzo, O. Ilbert, A. Iovino, F. Lamareille, H. J. McCracken, B. Marano, C. Mari-

- noni, A. Mazure, B. Meneux, R. Merighi, S. Paltani, R. Pellò, A. Pollo, L. Pozzetti, M. Radovich, D. Vergani, G. Zamorani, E. Zucca, M. Bondi, A. Bongiorno, J. Brinchmann, O. Cucciati, S. de La Torre, L. Gregorini, P. Memeo, E. Perez-Montero, Y. Mellier, P. Merluzzi, and S. Tempolin, *Astronomy and Astrophysics* **498**, 379 (2009), arXiv:0807.2578 [astro-ph].
- [49] M. G. Kitzbichler and S. D. M. White, *MNRAS* **391**, 1489 (2008), arXiv:0804.1965 [astro-ph].
- [50] J. Kormendy and L. C. Ho, *Annual Review of Astronomy and Astrophysics* **51**, 511 (2013), arXiv:1304.7762 [astro-ph.CO].
- [51] A. Sesana, A. Vecchio, and C. N. Colacino, *Mon. Not. Roy. Astron. Soc.* **390**, 192 (2008), arXiv:0804.4476 [astro-ph].
- [52] F. A. Marin *et al.* (WiggleZ), *Mon. Not. Roy. Astron. Soc.* **432**, 2654 (2013), arXiv:1303.6644 [astro-ph.CO].
- [53] A. Rassat, A. Amara, L. Amendola, F. J. Castander, T. Kitching, M. Kunz, A. Refregier, Y. Wang, and J. Weller, (2008), arXiv:0810.0003 [astro-ph].
- [54] G. Agazie *et al.* (International Pulsar Timing Array), *Astrophys. J.* **966**, 105 (2024), arXiv:2309.00693 [astro-ph.HE].
- [55] R. J. Truant, D. Izquierdo-Villalba, A. Sesana, G. Mohiuddin Shaifullah, and M. Bonetti, arXiv e-prints, arXiv:2407.12078 (2024), arXiv:2407.12078 [astro-ph.GA].
- [56] M. R. Sah and S. Mukherjee, (2024), arXiv:2407.11669 [astro-ph.CO].
- [57] M. Maggiore, *Gravitational Waves. Vol. 1: Theory and Experiments*, Oxford Master Series in Physics (Oxford University Press, 2007).
- [58] B. Allen, D. Agarwal, J. D. Romano, and S. Valtolina, *Phys. Rev. D* **110**, 123507 (2024), arXiv:2406.16031 [gr-qc].